



# Open Access Articles

## ***Activation of Sonic hedgehog signaling in neural progenitor cells promotes glioma development in the zebrafish optic pathway***

The Faculty of Oregon State University has made this article openly available.  
Please share how this access benefits you. Your story matters.

<b>Citation</b>	Ju, B., Chen, W., Spitsbergen, J. M., Lu, J., Vogel, P., Peters, J. L., ... & Taylor, M. R. (2014). Activation of Sonic hedgehog signaling in neural progenitor cells promotes glioma development in the zebrafish optic pathway. <i>Oncogenesis</i> , 3, e96. doi:10.1038/oncsis.2014.10
<b>DOI</b>	10.1038/oncsis.2014.10
<b>Publisher</b>	Nature Publishing Group
<b>Version</b>	Version of Record
<b>Terms of Use</b>	<a href="http://cdss.library.oregonstate.edu/sa-termsofuse">http://cdss.library.oregonstate.edu/sa-termsofuse</a>

## ORIGINAL ARTICLE

## Activation of Sonic hedgehog signaling in neural progenitor cells promotes glioma development in the zebrafish optic pathway

B Ju<sup>1</sup>, W Chen<sup>2</sup>, JM Spitsbergen<sup>3</sup>, J Lu<sup>4</sup>, P Vogel<sup>5</sup>, JL Peters<sup>6</sup>, Y-D Wang<sup>7</sup>, BA Orr<sup>5</sup>, J Wu<sup>1</sup>, HE Henson<sup>1</sup>, S Jia<sup>1</sup>, C Parupalli<sup>1</sup> and MR Taylor<sup>1</sup>

Dysregulation of Sonic hedgehog (Shh) signaling has been implicated in glioma pathogenesis. Yet, the role of this pathway in gliomagenesis remains controversial because of the lack of relevant animal models. Using the *cytokeratin 5* promoter, we ectopically expressed a constitutively active zebrafish Smoothed (Smoa1) in neural progenitor cells and analyzed tumorigenic capacity of activated Shh signaling in both transient and stable transgenic fish. Transient transgenic fish overexpressing Smoa1 developed retinal and brain tumors, suggesting *smoa1* is oncogenic in the zebrafish central nervous system (CNS). We further established stable transgenic lines that simultaneously developed optic pathway glioma (OPG) and various retinal tumors. In one of these lines, up to 80% of F1 and F2 fish developed tumors within 1 year of age. Microarray analysis of tumor samples showed upregulated expression of genes involved in the cell cycle, cancer signaling and Shh downstream targets *ptc1*, *gli1* and *gli2a*. Tumors also exhibited specific gene signatures characteristic of radial glia and progenitor cells as transcriptions of radial glia genes *cyp19a1b*, *s100β*, *blbp*, *gfap* and the stem/progenitor genes *nestin* and *sox2* were significantly upregulated. Overexpression of GFAP, S100β, BLBP and Sox2 was confirmed by immunofluorescence. We also detected overexpression of Mdm2 throughout the optic pathway in fish with OPG, therefore implicating the Mdm2–Tp53 pathway in glioma pathogenesis. In conclusion, we demonstrate that activated Shh signaling initiates tumorigenesis in the zebrafish CNS and provide the first OPG model not associated with neurofibromatosis 1.

*Oncogenesis* (2014) 3, e96; doi:10.1038/oncsis.2014.10; published online 31 March 2014

**Subject Categories:** Cellular oncogenes

**Keywords:** zebrafish; Sonic hedgehog (Shh) pathway; activated Smoothed (Smoa1); optic pathway glioma (OPG)

## INTRODUCTION

Hedgehog signaling is essential for many developmental processes including cell proliferation, differentiation and survival.<sup>1</sup> This biochemical pathway is highly conserved from *Drosophila* to mammals and is referred to as Sonic hedgehog (Shh) signaling in vertebrates. Shh functions as a mitogen for neural stem cells in the brain and retina, astrocyte precursor cells in the optic stalk and granule precursor cells in the cerebellum.<sup>2</sup> Dysregulation of this pathway in cerebellar granule neuron precursors causes the Shh subtype of medulloblastoma.<sup>3</sup> Increasing evidence also implicates this signaling pathway in other central nervous system (CNS) tumors, such as gliomas. For example, *in vitro* cell culture<sup>4</sup> and *in vivo* xenograft studies<sup>5,6</sup> revealed that Shh signaling pathway is essential for maintaining stem cells in a subset of gliomas. In addition, widespread overexpression of the *GLI1* transcription factor, a downstream activator of the Shh pathway, has been found in a panel of fresh brain tumors.<sup>5</sup> Activation of the Shh pathway is also common among pediatric pilocytic astrocytoma,<sup>7</sup> where a significant correlation exists between the Shh pathway components PTCH, GLI1 and the proliferation marker Ki67. Despite this evidence, it remains unclear whether Shh signaling activity drives glioma pathogenesis, partially because of the absence of relevant animal models.

In this study, we present a zebrafish model of Shh signaling-driven gliomagenesis in a subpopulation of neural progenitor cells in the optic pathway. We previously reported that constitutively active zebrafish Smoothed (Smoa1) is oncogenic in zebrafish, and its coexpression with the human constitutively active AKT1 leads to glioblastoma-like tumors in the brain, retina and spinal cord.<sup>8</sup> To examine whether overexpression of Smoa1 alone is sufficient to initiate tumorigenesis, we used the zebrafish *cytokeratin 5* (*krt5*) gene promoter to drive ectopic expression of Smoa1 in neural progenitor cells. We established stable transgenic lines that develop various retinal tumors and optic pathway glioma (OPG), herein referred to as zOPG. The zOPGs exhibit a radial glia and/or progenitor cell gene expression signature and overexpress Mdm2, a negative regulator of the Tp53 pathway. We propose that, at least in the context of zebrafish, activation of the Shh signaling pathway initiates gliomagenesis.

## RESULTS

The zebrafish *krt5* promoter drives transgenic expression in neural progenitor cells

Krt5 is a type II intermediate filament protein expressed in stratified epithelial cells of higher vertebrates and in neural cells of

<sup>1</sup>Department of Chemical Biology and Therapeutics, St Jude Children's Research Hospital, Memphis, TN, USA; <sup>2</sup>Department of Molecular Physiology and Biophysics, Vanderbilt University School of Medicine, Nashville, TN, USA; <sup>3</sup>Fish Disease Research Group, Department of Microbiology, Oregon State University, Corvallis, OR, USA; <sup>4</sup>Department of Pathology, National Center for Safety Evaluation of Drugs, National Institute for the Control of Pharmaceutical and Biological Products, Beijing, China; <sup>5</sup>Veterinary Pathology Core, St Jude Children's Research Hospital, Memphis, TN, USA; <sup>6</sup>Cell and Tissue Imaging, St Jude Children's Research Hospital, Memphis, TN, USA and <sup>7</sup>Computational Biology, St Jude Children's Research Hospital, Memphis, TN, USA. Correspondence: Dr MR Taylor, Department of Chemical Biology and Therapeutics, St Jude Children's Research Hospital, 262 Danny Thomas Place, Memphis, TN 38105, USA.

E-mail: michael.taylor@stjude.org

Received 25 October 2013; revised 11 February 2014; accepted 27 February 2014

lower vertebrates.<sup>9</sup> Expressed sequence tag analysis of zebrafish retinal tissues indicates that *krt5* mRNA is a prominent transcript in zebrafish retina, especially in the optic nerve.<sup>10</sup> For our study, we cloned a 4.9-kb fragment of the zebrafish *krt5* gene promoter and generated transgenic constructs to drive green fluorescent protein (GFP) expression that recapitulated the endogenous Krt5 expression pattern. In three independent *Tg(krt5:EGFP)* transgenic lines, GFP was expressed in the skin epithelium (Figure 1a), brain and retina (Figures 1b and g). In adults, GFP expression was found mainly in the brain ventricular zones (Figure 1c), where GFP-positive cells morphologically resembled radial glia cells that stained positive for the glial marker glial fibrillary acidic protein (GFAP, Figure 1d). GFP expression was also found in the hindbrain (Figure 1c), the optic tectum (OT, Figure 1c) and in reticular astrocytes of the optic nerve head (ONH, Figure 1e) and optic nerve (ON, Figure 1f). Based on the embryonic patterns of transgenic expression and radial glia cell morphology in the adult brain, we speculated that the GFP-positive cells within the brain and retina represent a population of neural progenitor cells.

As the Notch signaling pathway is involved in maintaining neural stem cells,<sup>11</sup> we predicted that inhibition of Notch signaling should result in loss of GFP-positive progenitor cells. To test this idea, we crossed our transgenic line to the zebrafish *mindbomb* mutant that is defective in Notch signaling due to an insertional mutation in *E3 ubiquitin ligase*.<sup>12</sup> Homozygous *mindbomb* mutants demonstrated a complete loss of GFP expression within the brain parenchyma and retina, whereas the expression in skin epithelium was not affected ( $n=4$ , Figures 1g and h). This result indicates

that Krt5 is a downstream target of Notch signaling in the zebrafish CNS and that the *krt5* gene promoter drives transgenic expression in neural progenitor cells.

#### Smoa1 is oncogenic in the zebrafish CNS

We adapted the *Gal4VP16-UAS* bigenic transgenic system<sup>8</sup> to ectopically express Smoa1-EGFP under control of the *krt5* promoter (Figure 2a). In transient transgenic conditions, ~8% (7/90) of adult fish developed either microphthalmia (Supplementary Figure 1a) or gross retinal tumors (Supplementary Figure 1b) at ~6 months of age. Histological analysis revealed these fish had either retinal dysplasia (Supplementary Figure 1a') or glioma-like tumors (Supplementary Figures 1b' and b''), respectively.

To examine whether other zebrafish CNS-specific gene promoters, such as *nestin* and *gfap*,<sup>13</sup> could drive Smoa1 tumorigenesis, we generated similar DNA constructs with these two promoters. In transient transgenic fish, we observed a fish with retinal tumor and another with a brain tumor when the *nestin* promoter was used (2/59, 3.4%; Supplementary Figures 1c and c'). We observed two fish with retinal tumors when the *gfap* gene promoter was used (2/38, 5.3%), including a case of medulloepithelioma (Supplementary Figures 1d and d'). Stable transgenic fish carrying these two DNA constructs were embryonic lethal, and hence tumor spectrum in adult fish is unknown.

From 90 F0 fish carrying the *krt5*-driven transgenic construct, we identified 10 stable transgenic lines. Six lines expressed the transgene prominently in the skin epithelium, and none of them developed tumors throughout their lives. Four additional lines

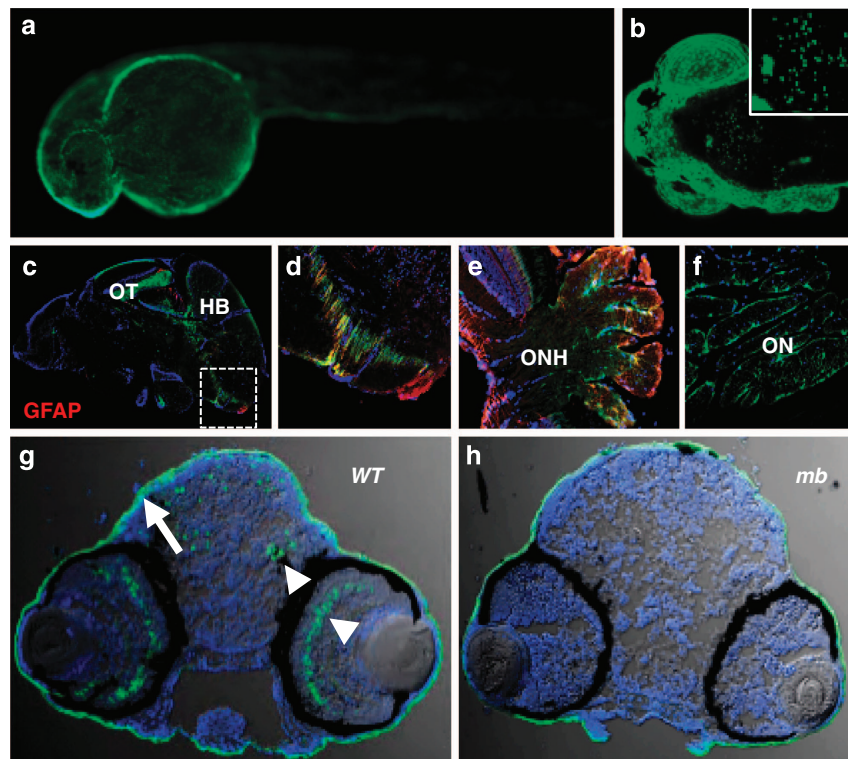


**Figure 1.** GFP expression patterns in the *Tg(krt5:EGFP)* line. (a) Skin epithelia expression in a 24 h.p.f. embryo (side view, anterior to the left). (b) Confocal imaging of GFP-positive cells in the brain of a 72 h.p.f. larva (dorsal view, anterior left). (c) Sagittal cryosection of an adult fish brain showing GFP expression in the ventricular zones, the OT and the hindbrain (HB). (d) Zoomed-in view of the white frame in (c) showing GFP-positive cells in the ventricular zones resembling radial glia cells partially positive for GFAP (red). (e) GFP expression in the ONH showing little overlap with the retinal Müller glial marker GFAP (red). (f) GFP expression in the reticular astrocytes of the ON. (g) Transverse section through the brain region of a wild-type (WT) 72 h.p.f. larva showing GFP expression in the skin (arrow), brain and retina (arrowheads). (h) GFP expression in the brain and the retina was absent in the *mindbomb* (*mb*) mutant background, whereas expression in the skin was not affected. All cryosections were counterstained with 4',6'-diamidino-2-phenylindole (DAPI) to label nuclei (blue).

showed varying levels of expression in the brain and retina, and displayed retinal abnormalities at variable penetrance. We characterized one line in detail, *Tg(krt5:Gal4VP16;14 × UAS-smoa1-EGFP)<sup>sj4</sup>*, that expressed the highest level of the transgene in the CNS, and therefore had the highest tumor incidence.

Embryos from this stable line began to express GFP at 16 h post fertilization (h.p.f.), and expression became prominent in the forebrain and retinal neuroblasts at 24 h.p.f., but no noticeable expression in skin epithelium was observed (Figure 2b and Supplementary Figure 2a). GFP expression was restricted to the retina and the ON at 96 h.p.f. (Figure 2c). To verify that this expression pattern was driven by the *krt5* gene promoter, we crossed this transgenic fish to another line, *Tg(UAS-E1b:nfsB-mCherry)<sup>c264</sup>*, that carries the upstream activation sequence (UAS) that can be activated by the Gal4VP16 fusion protein in our stable line (Figure 2a).<sup>14</sup> We observed mCherry expression in the forebrain, the optic stalk and retinoblasts in the double transgenic fish (Figure 2d). More importantly, we also observed mCherry expression in skin epithelium (Supplementary Figure 2b),

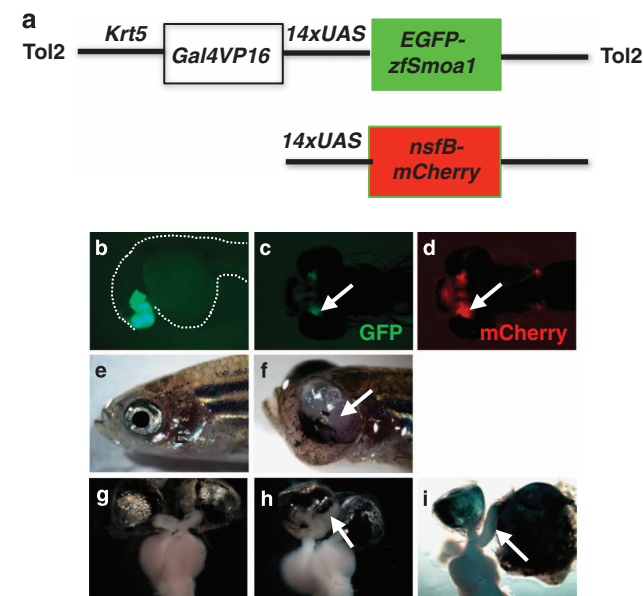


**Figure 2.** Phenotypic characterization of a stable transgenic line. (a) Graphic representation of the DNA constructs used for transgenesis and breeding. (b) A 24 h.p.f. embryo expresses Smoa1-EGFP in the forebrain and retinal neuroblasts. A 96 h.p.f. double transgenic embryo derived from crossing of the *Tg(krt5:Gal4VP16;14 × UAS:smoa1-EGFP)* and the *Tg(UAS-E1b:nfsB-mCherry)<sup>c264</sup>* stable lines expressed GFP (c) and mCherry (d) in the ONs (arrows). (e) A 6-month-old wild-type and (f) a transgenic fish with a gross tumor in its left eye (arrow). (g) Wild-type fish formed a normal optic chiasm, whereas (h) transgenic fish failed to form optic chiasm and showed dramatic expansion of the ONH region (arrow). (i) Dissected brain and eyes showing an enlarged ON associating with a gross eye tumor (arrow).

indicating that the expression of the oncogenic Smoa1-EGFP was indeed driven by the *krt5* promoter.

Transgenic embryos expressing high levels of GFP exhibited a coloboma phenotype at 96 h.p.f. (Supplementary Figure 2d). Cryosections of these larvae revealed that the choroid fissure failed to close (Supplementary Figure 2d', *n* = 6), a phenotype resembling zebrafish *ptc1* mutant.<sup>15</sup> Histological examination of 1- to 2-week-old larvae showed retinal lamination defects and ectopic retinal proliferation, especially at the ciliary marginal zones (Supplementary Figure 2e, *n* = 4), a phenotype reminiscent of the zebrafish *ptc2* mutants (the ortholog of the mammalian *Ptch1*).<sup>16</sup> Occasionally, even adult fish eye exhibited characteristics of human coloboma (Supplementary Figure 2f). Thus, our stable transgenic fish recapitulate phenotypic features of zebrafish Shh pathway activation.

Eye defects became noticeable in juveniles at 1 month of age. These fish had darker than usual eyes. As the F1 fish grew, they began to develop gross eye tumors starting at ~ 2 months, either unilaterally or bilaterally. Approximately 80% of F1 and F2 fish developed gross eye tumors by 1 year of age (Figures 2e and f), when most fish were killed because of heavy tumor burden. Surprisingly, transgenic fish showed no significantly higher mortality compared with controls during the first year of their life. However, most became darker in pigmentation and noticeably thinner, likely because of poor visual perception and malnutrition. We dissected > 50 adult F1 and F2 fish with retinal abnormalities, ranging from 2 to 12 months of age. These fish usually had significant expansion of the ONH that manifested as white masses that invaded neural retinae (Figures 2g and h). Optic nerves projected correctly to the contralateral optic tectums, but they failed to form optic chiasmata (*n* = 56, Figure 2h). In fish with unilateral eye tumors, the ON associated with the gross eye tumor was often larger (67%, *n* = 12/18, Figure 2i).

Activation of Shh pathway results in retinal dysplasia and retinal tumors

We performed transverse paraffin sectioning on 35 F1 and F2 fish with eye tumors ranging from 4 months to 1 year of age (Table 1). Histological analyses revealed two distinct populations of cells in nearly every tumor, originating from the neural retina or from the ONH respectively, consistent with our observation in dissected eye tumors. The neural retina-derived tumors usually exhibited high cellularity, whereas the ONH-derived region showed low to mild hypercellularity (Figures 3a and a' and 4). Five fish with relatively minor eye abnormalities showed disorganized retinal structures with occasional rosette structures (Figure 3a'). We refer to this phenotype as retinal dysplasia because of the histological similarity to a common yet poorly understood human retinal condition.<sup>17</sup> Although less affected retinae only showed localized retinal patterning defects, fish with gross eye tumors usually lost their laminated structures completely and exhibited distinct histopathological features of various ocular tumors. We found two cases that were morphologically similar to human medulloepithelioma with characteristic neural tube structures

Table 1. Tumor spectrum from histopathological analysis of 35 stable F1 and F2 transgenic fish with retinal tumors					
Tumor type	OPG	Medulloepithelioma <sup>a</sup>	Ocular melanoma <sup>a</sup>	Retinal PNET <sup>a</sup>	Brain tumor <sup>b</sup>
Tumor number	34	2	5	21	1
Ratio (percentage)	97.1	5.7	14.3	60	~ 1

Abbreviations: OPG, optic pathway glioma; PNET, primitive neuroectodermal tumor. <sup>a</sup>Nearly all fish developed OPG, except for one fish with ocular melanoma only. <sup>b</sup>This fish had concurrent OPG, ocular melanoma and hindbrain glioma, and was the only fish out of 92 F2 adult fish that developed a brain tumor.



(Figures 3b and b'), and five cases similar to human pigmented ocular melanoma with heavy pigmentation and bland nuclei (Figures 3c and c'). The majority of other tumors were collectively referred to as primitive neuroectodermal tumors (Figures 3d and d').

Activation of Shh pathway results in zOPG development

Out of the 35 fish analyzed histologically, 9 were sectioned through the entire optic pathway at various planes. Increased ON diameters associated with hyperplasia were found in either one or both optic nerves of these fish (Figures 4a and b). In the affected

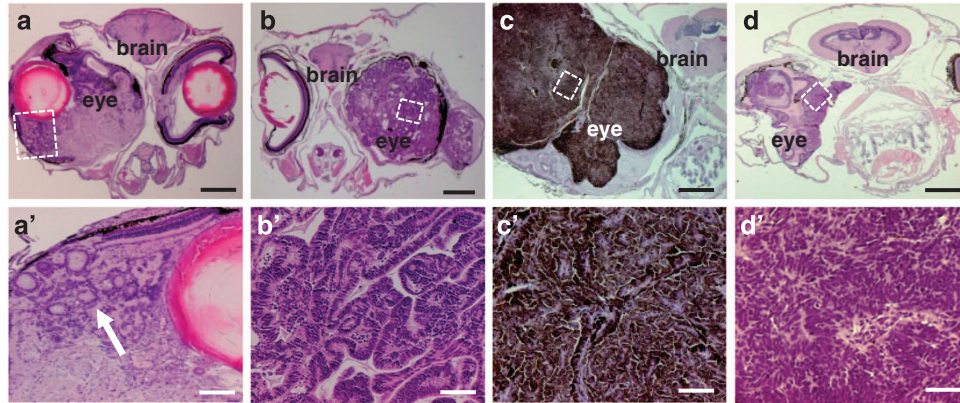


**Figure 3.** Retinal tumors resulted from expression of Smoa1-EGFP in the stable transgenic line. (a, a') Hematoxylin and eosin (H&E) staining of transverse section of a fish with retinal dysplasia; note the formation of rosette-like structures (arrow). (b, b') An ocular tumor resembling medulloepithelioma with characteristic neural tube structures. (c, c') A tumor showing features of pigmented ocular melanoma with heavy pigmentation and bland nuclei. (d, d') An adult fish developed unilateral primitive neuroectodermal tumor (PNET). White frames indicate areas that were enlarged (not to scale). Scale bars, 400  $\mu\text{m}$  for (a–d), 40  $\mu\text{m}$  for (a'–d'), respectively.

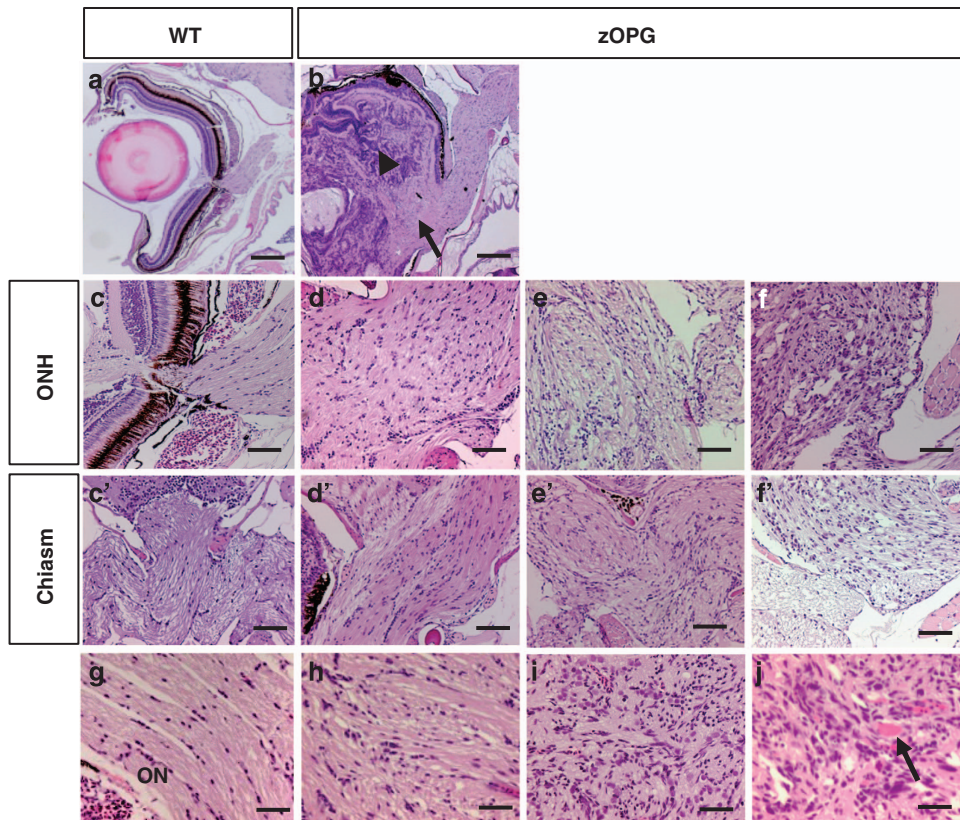


**Figure 4.** Stable transgenic fish developed zOPGs. (a) Hematoxylin and eosin (H&E) staining of paraffin sections from a wild-type (WT) adult retina, and (b) an eye tumor showing coexistence of retinal dysplasia and ON hyperplasia. Note the high cellularity originating from the neural retina (arrowhead) and low cellularity derived from ON (arrow). (c) Enlarged view of normal ONH showing low cellularity, and transgenic fish show ON hyperplasia to neoplasia (d–f). (c') Enlarged view of a normal optic chiasm showing low cellularity, and transgenic fish showing disorganization and increased cellularity in chiasms (d'–f'). (g) High-magnification view of a normal ON showing low cellularity, with zOPGs showing increased cellularity, nuclear atypia and vascular proliferation (h–j, arrow). Scale bars, 200  $\mu\text{m}$  for (a and b), 40  $\mu\text{m}$  for (c–f') and 20  $\mu\text{m}$  for (g–j), respectively.

optic nerves, hyperproliferation was evident throughout the optic pathway, affecting not only the ONH (Figures 4c–f), but also the optic chiasm and the distal optic tract (Figures 4c'–f'). The most pronounced hyperproliferation occurred at the ONH, with presumptive glial cells in this region proliferating, expanded into, and sometimes mixed with neural retinal cells. When observed at high magnification, the ONH-derived tumors showed nuclear pleomorphism with scattered atypical nuclei, characteristic of low-grade gliomas (Figure 4h). Occasionally, tumors with high cellularity and microvascular proliferation were also observed (Figures 4i and j), suggesting tumors of higher grades. Overall, from analysis of paraffin sections and observation of brain dissections, nearly every adult fish with gross eye tumor developed optic pathway tumors.

zOPGs exhibit radial glia or neural progenitor cell signatures

To gain a comprehensive view of the gene transcriptional profiles, we performed microarray analysis of gross eye tumors vs age-matched wild-type fish eyes ( $n=4$  per group). Gene Ontology analysis identified 1901 differentially expressed genes, with the most downregulated genes involving visual perception and the most upregulated genes involving cell cycle (Figure 5a and Supplementary Figure 3a). Up-regulation of *gli1*, *gli2a*, *gfap*, and *wnt5a* was confirmed by real-time quantitative PCR (Figure 5b). KEGG (Kyoto Encyclopedia of Genes and Genomes) pathway analyses revealed significant upregulation of pathways in cancer, such as those for basal cell carcinoma, glioma and small-cell lung cancer and the cell cycle (Supplementary Figure 3a). Consistent with the upregulation of genes involved in the cell cycle, we found

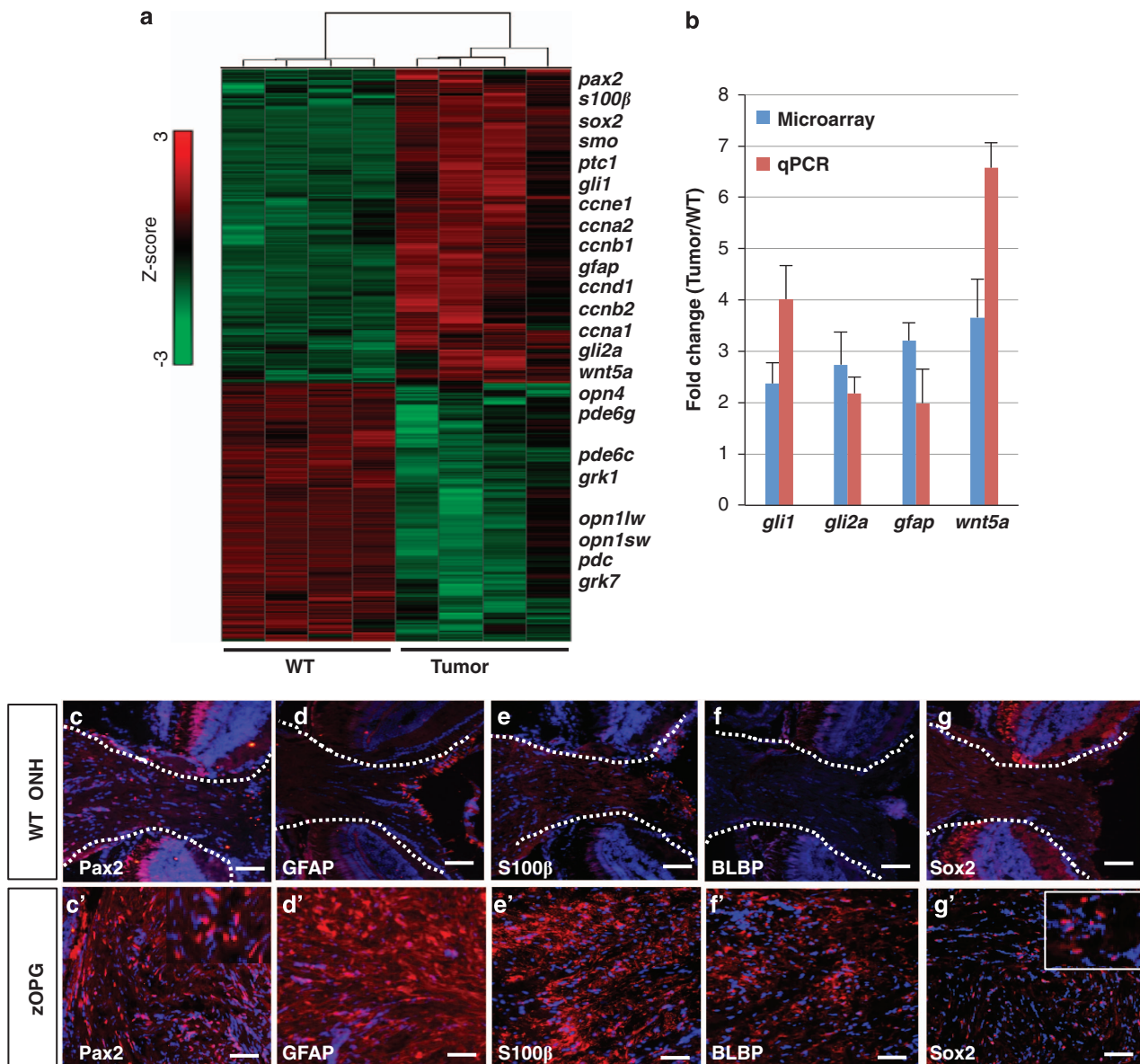


**Figure 5.** Differentially expressed genes and a radial glia cell signature of the zOPGs. (a) A heatmap generated by hierarchical clustering showing differentially expressed genes for wild-type (WT) and retinal tumors, respectively. The color scale (Z-score) is denoted on the right, with red showing upregulation and green showing downregulation. A subset of upregulated genes is listed on the right. (b) Upregulation of *gli1*, *gli2a*, *gfap* and *wnt5a* was confirmed by real-time quantitative PCR (qPCR). Microarray data represent the average expression from four eye tumors versus four control eyes. qPCR data are from the same four samples performed in quadruplicate. All data were normalized to *actin b1* expression. Error bars show s.d. (c–g') Series of cryosections from a single fish with typical zOPG showed overexpression of the astrocyte/radial glia markers of Pax2 (c, c'), GFAP (d, d'), S100β (e, e'), BLBP (f, f') and the stem cell and glioma marker Sox2 (g, g') as compared with their respective expression in the ONH of an age-matched WT fish. Fragmented lines demarcate the ONH region. Scale bars, 40 μm.



a significant increase in the mitotic index by phospho-histone H3 staining of transgenic larval retinae at 5 days post fertilization and of adult retinal glial tumors (Supplementary Figures 3b–f). We also examined these samples for apoptosis using an anti-active caspase 3 antibody that we confirmed to stain prominently and specifically in 72 h.p.f. larval brain and retinae treated with the cyclin-dependent kinase inhibitor, Roscovitine.<sup>18</sup> We found no detectable apoptotic activity in retinal tumors ( $n=8$ ; data not shown).

As ONH-derived putative glioma constituted the bulk of most tumors, we analyzed transcriptional profiles of genes expressed by astrocytes or radial glia. Array data showed a moderate increase in *gfap* and a high increase in *s100 $\beta$*  transcription (Supplementary Figure 4). We also discovered an ~10-fold upregulation of the radial glial marker *fabp7a* (brain fatty acid binding protein 7a, equivalent to human *BLBP*) and nearly a 60-fold increase in another zebrafish radial glia marker *cyp19a1b* (brain aromatase B). Not surprisingly, transcription of the stem cell markers of *nestin* and *sox2* were also significantly upregulated.

To distinguish differential gene expression in neural retina-derived tumors vs ONH-derived glial tumors and to confirm the glial identity of the latter, we performed immunofluorescence on cryosections from typical retinal tumors with gross ONH expansion using several well-known glial cell markers ( $n=12$ ). The two tumor types in individual samples were easily distinguishable on 4',6-diamidino-2-phenylindole-stained cryo- or paraffin-sections as neural retinal tumors always showed dense cluster of nuclei, whereas glial tumors were usually sparsely nucleated. We first analyzed Pax2 expression, because *pax2* is a known target of Shh signaling at the optic stalk in zebrafish<sup>15</sup> and mouse<sup>19</sup> eye development, and Pax2 expression is specific to a subset of ON astrocytes in adults. We observed Pax2-positive cells evenly

distributed in the putative glial tumors, but never in neural retinal tumors (Figures 5c and c'). This observation is consistent with the microarray data (Figure 5a) and further supports ONH origin of the glial tumors. The glial tumors also showed overexpression of GFAP (Figures 5d and d'), S100 $\beta$  (Figures 5e and e') and BLBP (Figures 5f and f'). We also examined the expression of the neural stem cell marker Sox2 that has recently been found to be a novel glioma-associated antigen.<sup>20</sup> Immunofluorescence revealed Sox2 in glial tumors with characteristic nuclear expression (Figures 5g and g',  $n=6$ ). Collectively, overexpression of Cyp19a1b, S100 $\beta$ , BLBP, GFAP, Nestin and Sox2 reflects the unique zebrafish stem cell niche of the adult telencephalic ventricular zone.<sup>21</sup> Whether this radial glia and progenitor cell expression signature of the zOPG was inherited from the tumors' cell of origin or acquired during the course of tumorigenesis warrants further study.

#### Activation of Shh pathway results in OT asymmetry and brain tumorigenesis

Wild-type zebrafish exhibit symmetrical brain development, as exemplified by the prominent OT (Figure 6a). Observation of dissected brains from eye-tumor-bearing transgenic fish revealed asymmetric development of the OT in most cases (78%,  $n=14/18$ ). The tectal lobes associated with gross eye tumors were usually larger than the contralateral lobes that were associated with less affected eyes (Figure 6b). Statistical analyses confirmed the significant difference in OT of transgenic fish, but not of wild-type fish (Figure 6c). We also observed spiraling or spinning swimming behavior in 8 out of 92 F2 transgenic fish between the ages of 6 and 12 months. One fish showed a bump in the head (Figure 6d). Hematoxylin and eosin staining of transverse paraffin

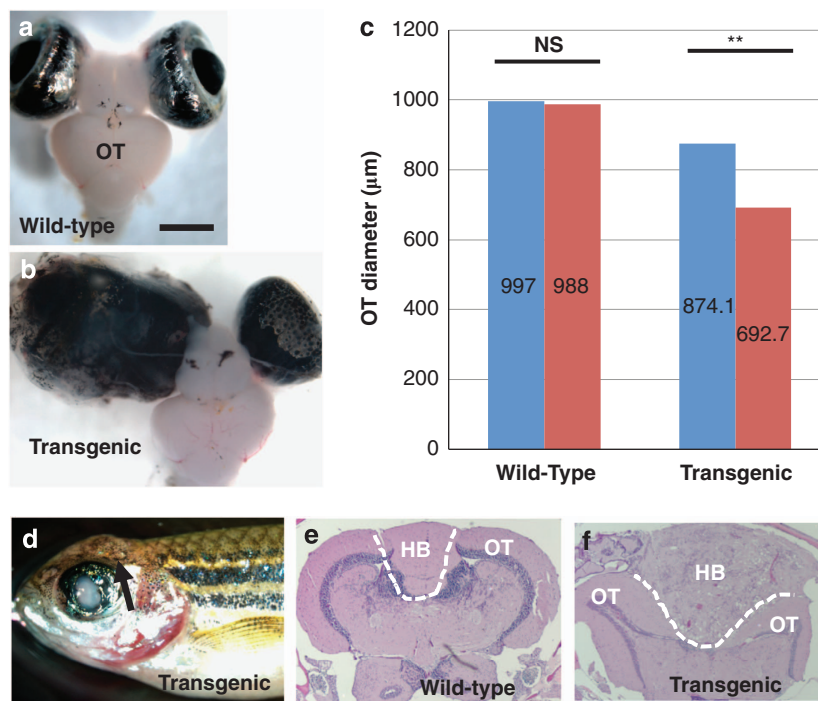


**Figure 6.** Stable transgenic fish exhibited asymmetric OT development and brain tumorigenesis. (a) A wild-type adult fish exhibited symmetric development of OT, scale bar, 1000  $\mu\text{m}$ . (b) A transgenic fish with gross eye tumor exhibited asymmetric OT development. (c) Comparison between left (blue bar) and right (red bar) tectal lobe diameters in the wild-type fish and between larger (blue bar) and smaller (red bar) tectal lobes in the transgenic fish showed significant difference in transgenic fish OT, but not in wild-type fish OT ( $n=10$ ). NS, statistically not significant;  $**P<0.01$ . Error bars show s.d. In general, the OT from transgenic fish was smaller than wild type, because the tumor-bearing fish were smaller. (d) A 12-month-old transgenic fish showing a brain tumor (arrow); (e) hematoxylin and eosin (H&E) staining of a transverse section at the boundary of the OT and hindbrain (HB) from a wild-type fish showing symmetric OT and a small hindbrain area. (f) H&E staining of the brain tumor in (d) showing tumor formation in the HB.

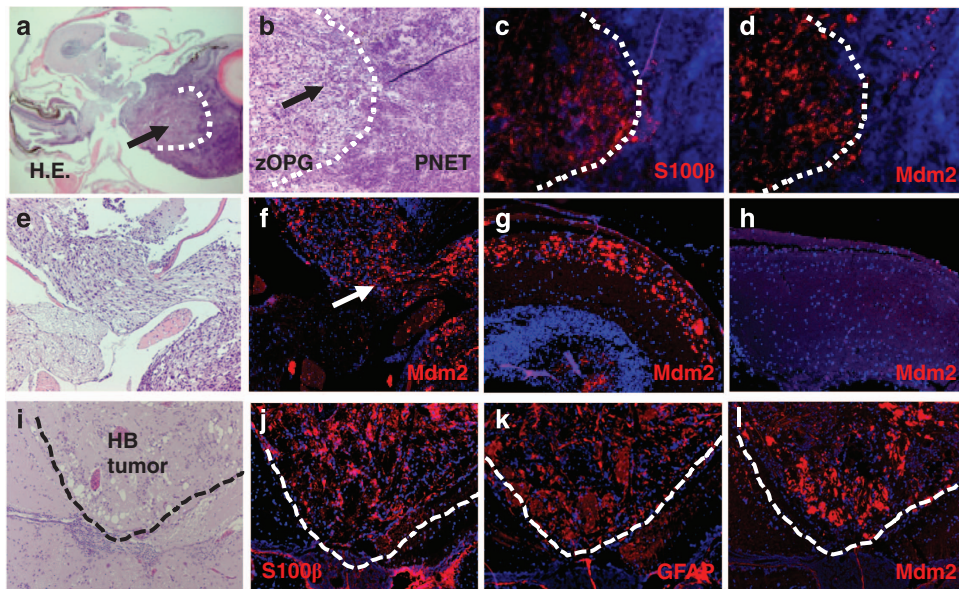


**Figure 7.** Overexpression of Mdm2 in zOPGs and hindbrain tumor. (a) Hematoxylin and eosin (H&E) staining of a transverse section from an adult fish with a less affected eye and a gross eye tumor (arrow). (b) A fragmented line demarcates the zOPG with mild cellularity and a primitive neuroectodermal tumor (PNET) with high cellularity. Immunofluorescence revealed that only the zOPG exhibited S100 $\beta$  (c) and Mdm2 (d) overexpression, whereas the PNET did not. (e) H&E-stained transverse section showing the optic chiasm of the same fish. Mdm2 was only expressed in the optic nerve associated with the glioma (f, arrow). (g, h) High-magnification view of the two optic tectal lobes in (a) showing Mdm2 expression in the lobe associated with zOPG (g), but not in the contralateral lobe (h). (i) H&E staining of the hindbrain tumor. The tumor overexpressed radial glia markers S100 $\beta$  (j), GFAP (k) and Mdm2 (l).

sections indicated the fish had a hindbrain tumor that is histopathologically similar to zOPGs (Figures 6e and f). These observations of abnormal brain development conform to studies suggesting that Shh signaling acts as a mitogen to modulate neural progenitor proliferation in both mouse dorsal brain<sup>22</sup> and zebrafish optic tectum.<sup>23</sup>

#### zOPG development is associated with Mdm2 overexpression

The TP53 tumor-suppressor pathway is frequently involved in the pathogenesis of the most severe type of human glioma, glioblastoma.<sup>24</sup> Recent reports indicate that SHH signaling could negatively modulate the TP53 pathway through MDM2 activation. For example, MDM2 is activated in several human breast cancer cell lines that express the SMO-M1 and SMO-M2, the two activating mutations of SMO.<sup>25</sup> MDM2 overexpression has also been observed *in vivo* in the P0 mouse brain overexpressing the full-length *Gli1*.<sup>26</sup> To determine whether zebrafish *Smoa1* could upregulate Mdm2, we analyzed Mdm2 expression in tumor samples. Following an extensive analysis on both cryosections and paraffin sections of gross eye tumors, we found widespread expression of Mdm2 in the zOPGs, but not in other retinal tumors ( $n=22$ , Figure 7 and Supplementary Figure 5a).

Immunofluorescence revealed Mdm2 expression in retinal Müller glial cells of the ONH from wild-type fish retinae, overlapping expression of GFAP (Supplementary Figure 5b,  $n=4$ ). This raised the issue of whether the presence of the Mdm2-positive cells in glioma is simply a reflection of expanding Mdm2-positive cells at the ONH or whether Mdm2 plays a larger role in gliomagenesis. To address this concern, we took advantage of fish with OT asymmetry associated with zOPG development and analyzed Mdm2 expression patterns in these asymmetrical OTs (Figure 7a). As expected, Mdm2 was overexpressed in the glial tumor mass (Figures 7b–d,  $n=7$ ). Unexpectedly, in five out of the seven samples, Mdm2 expression was not restricted to the tumor mass at the ONH, but was found throughout the optic pathway, including the optic tracts, the chiasm (Figures 7e and f) and the OT

(Figure 7g and Supplementary Figure 5c). Mdm2 expression in these components of the pathway was not detectable in wild-type fish. In fact, even the relatively normal contralateral side of the same fish showed either no or little Mdm2 expression (Figures 7f and h and Supplementary Figure 5c). To verify the specificity of the antibody, we further blocked Mdm2 staining using the immunizing peptide (Supplementary Figure 3d). Analysis of the single hindbrain tumor (Figures 6d and 7i) showed that it overexpressed S100 $\beta$  (Figure 7j) and GFAP (Figure 7k), therefore confirming its glioma identity. This hindbrain glioma also overexpressed Mdm2 (Figure 7l). The zOPG, asymmetrical OT and brain tumor-specific Mdm2 overexpression suggests a conserved role for Mdm2 in modulating zebrafish CNS development and potentially tumor pathogenesis. Whether this Mdm2 overexpression resulted directly from Shh pathway activation or was the consequence of tumorigenesis and what precise roles Mdm2 had played in the tumorigenesis process are the subjects for further investigation.

#### DISCUSSION

In this study, we developed the first animal model of gliomagenesis driven by Shh activation. We identified a *krt5* promoter sequence that targeted oncogenic *Smoa1* expression to putative neural progenitor cells in the zebrafish CNS. Using both transient expression and stable transgenic lines, we provide strong evidence that activated Shh signaling initiates zOPG and other CNS tumors in zebrafish. The zOPGs exhibit a radial glia and progenitor cell gene expression signature, a feature of both low-grade<sup>27</sup> and aggressive gliomas.<sup>28</sup> In addition, these tumors overexpressed Mdm2, supporting recent findings<sup>25,26</sup> that SHH activates MDM2. Our results further demonstrate a potential interaction between SHH signaling and the TP53 pathway in glioma pathogenesis.

#### Shh signaling and defective retinal development

Association of activated SHH signaling with retinal defects have been shown in human Gorlin's syndrome patients,<sup>29</sup> in



heterozygous *Ptc* +/− mice<sup>30</sup> and in zebrafish *ptc2* mutants.<sup>16</sup> As homozygous *Ptc1* −/− mice die early in embryonic development, and very few zebrafish *ptc2* mutants survive to adult stage, the effects of aberrant Shh signaling on retina development is not fully understood and observations in humans have been limited to minor retinal dysplasia with anecdotal human ocular tumor correlation.<sup>31</sup> SHH signaling is known to exert positive roles for retinal progenitor cell proliferation through regulation of cell cycle targets across species.<sup>32,33</sup> For example, mouse *Smo* −/− cKO mutants show reduced transcripts of *cyclin A2*, *cyclinB1*, *cyclin D1* and *cyclin E* in the retina.<sup>34</sup> In addition, studies performed in *Xenopus* suggest that Shh activation accelerates cell cycle and transforms retinal stem cells to faster cycling progenitors that may contribute to tumor initiation and progression.<sup>35</sup> A recent study further shows that Shh signaling promotes not only proliferation but also cell survival in zebrafish retina.<sup>36</sup> The combined proliferation and pro-survival activities of a sustained Shh signaling may have collectively contributed to retinal tumorigenesis.

### Shh signaling and gliomagenesis

Despite the correlation between SHH target gene expression and glioma,<sup>7,22</sup> as well as the strong evidence that SHH signaling is essential for glioma stem cell proliferation, self-renewal and tumorigenesis,<sup>4,5</sup> dysregulation of SHH signaling had not previously been shown to be sufficient for glioma initiation and maintenance in an animal model. The only direct *in vivo* evidence correlating activated Shh signaling with brain tumorigenesis comes from injection of *GLI1* mRNA into the dorsal animal pole of frog embryos, leading to neural tube hyperplasia.<sup>22</sup> More recently, it was shown that overexpression of *SmoM2* in mouse Olig2-positive cells resulted in ventral pon hypertrophy, suggesting that dysregulated Shh signaling plays a role in the pathogenesis of diffuse intrinsic pontine glioma. However, dysplasia was absent in this model, indicating that Shh dysregulation alone is insufficient for gliomagenesis.<sup>37</sup> Our results suggest that activated Shh signaling in zebrafish not only led to asymmetric OT development, but also zOPG. These tumors exhibited gene expression signatures of basal cell carcinoma and small-cell lung cancer, both involving dysregulation of the Shh pathway (Supplementary Figure 3a).<sup>38</sup> Therefore, our study provides the first *in vivo* model associating activated Shh signaling with gliomagenesis. So, why are zebrafish apparently more prone to developing glioma from aberrant Shh signaling? We hypothesize that the following factors might play a role: (1) lack of a functional ARF (alternative reading frame) tumor-suppressor gene in lower vertebrates,<sup>39</sup> such as zebrafish, could enhance the overall tumorigenicity in certain tissues or organs; (2) zebrafish possess abundant neural stem cells and proliferation zones throughout the CNS,<sup>40</sup> providing a fertile environment for oncogene-induced tumorigenesis; and (3) the ONH, with its unique glial features that facilitate continued growth, including a rich blood vasculature,<sup>41</sup> may represent a stem or progenitor cell niche and provide a permissive context<sup>42</sup> for gliomagenesis from constitutive Shh signaling. We believe other niches susceptible to Shh-induced gliomagenesis also exist within the zebrafish CNS, and our preliminary results support this presumption.

The zOPGs and hindbrain tumors were low-grade gliomas that exhibited low cellularity and lacked intratumor necrosis. In contrast, our previous study showed that zebrafish developed gliomas with features of human glioblastoma when coexpressing zebrafish *Smoa1* and the constitutive human AKT1.<sup>8</sup> In fact, a more recent study indicated that activation of Shh and phosphoinositide 3-kinase promotes human glioblastoma growth,<sup>38</sup> suggesting a conserved mechanism of gliomagenesis across species. Interestingly, we did not detect phospho-AKT (Ser473) or phospho-AKT (Thr308) expression in our tumor

samples ( $n=8$ , data not shown), indicating that additional oncogenic pathways may play a role in glioma progression. Consistent with this idea, we found that Mdm2 was upregulated in our tumor samples.

### Shh signaling and optic pathway glioma

In human, optic pathway gliomas are pediatric CNS tumors of glial cell origin and are associated with *neurofibromatosis 1* (*NF1*) mutations.<sup>43</sup> Although children carrying *NF1* mutations account for ~50% of OPG cases, the etiology of non-*NF1* OPG remains unknown.<sup>44</sup> Our study indicates that upregulated Shh signaling may promote overproliferation and tumorigenesis in the optic pathway, and this is in agreement with evidence supporting a mitogenic role for Shh signaling in glial precursor cells of the mammalian optic nerve.<sup>19,45</sup> However, OPGs have not been reported in human patients with Gorlin's syndrome because of mutation of the *Patched1* gene, although some patients show abnormal glial proliferation around the ONH.<sup>29</sup> It is worth noting that when Shh signaling is activated in the zebrafish optic pathway, the area most susceptible to tumorigenesis is the ONH. Thus, it would be interesting to determine whether activated Shh signaling plays a role in causing a subset of non-*NF1* OPGs.

In summary, our study expands the current knowledge of tumorigenesis resulting from dysregulation of Shh signaling and may contribute to the understanding of the cell origins and molecular mechanisms of CNS tumors, particularly gliomas. In light of our results and recent insights into potential new treatments for human melanoma<sup>46</sup> and leukemia<sup>47</sup> provided by zebrafish studies, zebrafish may become a cost-effective model for validating candidate glioma oncogenes identified through human genome sequencing while providing an appealing *in vivo* platform to screen for drugs that treat certain tumors of the CNS.

## MATERIALS AND METHODS

### Zebrafish husbandry

AB and *Tg(UAS-E1b:nfsB-mCherry)*<sup>264</sup> strains were acquired from the Zebrafish International Resource Center (ZIRC, Eugene, OR, USA). Embryos and larvae were maintained at 28.5 °C in egg water (0.03% Instant Ocean, Blacksburg, VA, USA). All experiments were conducted in accordance with the St Jude Children's Research Hospital Institutional Animal Care and Use Committee.

### DNA constructs

A 4971-bp fragment of the zebrafish *krt5* promoter (accession no. KC857549) was inserted into the 5' entry clone *p5E-MCS* from the Multisite Gateway-compatible entry vectors of the Tol2 kit.<sup>48</sup> The *Gal4VP16;14 × UAS-smoa1-EGFP* fragment was inserted into the middle entry clone *pME-MCS*. The p5E and pME vectors containing the respective promoter and oncogenic sequences were combined with the 3' entry clone *p3E-polyA* and the destination vector *pDestTol2pA2* to create the construct *pKrt5:Gal4VP16;14 × UAS-smoa1-EGFP* using the LR Clonase II Plus Enzyme mix (Invitrogen, Carlsbad, CA, USA). The construct was coinjected with Tol2 transposase mRNA into one-cell stage embryos. Embryos were raised to adulthood and screened for germline transmission.

### Immunohistochemistry

Immunofluorescence on paraffin sections and cryosections was conducted following the protocol from Cell Signaling Technology (Danvers, MA, USA). The following rabbit polyclonal antibodies of Mdm2 (Anaspec, Fremont, CA, USA, 55470, 1:200; Blocking peptide 55470P), Pax2 (Covance, Nashville, TN, USA, PRB-276P, 1:1000), S100 (Dako, Glostrup, Denmark, Z0311, 1:2000), Sox2 (Millipore, Billerica, MA, USA, AB5603, 1:500), GFAP (Dako, Z0034, 1:1000), BLBP (Millipore, ABN14, 1:200), phospho-Histone 3 (Ser10) (Cell Signaling, 9701, 1:100), active Caspase 3 (Cell Signaling, 9661, 1:200) and mouse monoclonal antibodies of GFAP (Sigma, St Louis, MO, USA, G6171, 1:400) were used. Fluorescence images were taken either on an Olympus IX81 fluorescent microscope using Olympus

DP Controller software (Olympus, Center Valley, PA, USA) or on a Nikon TE2000E2 microscope equipped with Nikon C1Si confocal using Nikon NIS Elements, (Nikon, Melville, NY, USA).

### Microarray and data analysis

Total RNA at 200 ng was amplified and labeled using an Agilent Low Input Quick Amp kit (5190-2305). Microarray was performed using Agilent-026437 (Agilent, Santa Clara, CA, USA), Zebrafish GX v3 4 × 44K (Santa Clara, CA, USA) according to the manufacturer's recommendations. Microarrays were scanned with an Agilent scanner (G2565CA) at 3 μm resolution, and data were extracted by Agilent Feature Extraction software (v.10.5.1.1) using GE1\_105\_Jan09 protocol. Quantile normalization on background-subtracted signal intensity was performed among the samples, and a *P*-value using *t*-test was calculated for each gene as statistical measurement of the replicates. The selection of significant genes was based on at least a twofold change and a probability of >95% (*P* < 0.05) on differential expression among the four replicates.

### Real-time reverse transcription-PCR

Total RNA was reverse transcribed (SuperScript VILO cDNA Synthesis Kit, Invitrogen) and real-time PCR was performed using the TaqMan Fast Advanced Master Mix (Applied Biosystems, Grand Island, NY, USA). Probes for PCR were: *actinb1* (Dr03432610\_m1), *gli1* (Dr03093665\_m1), *gli2a* (Dr03144185\_m1), *gfap* (Dr03079975\_m1) and *wnt5a* (Dr03123879\_m1) (Life Technologies, Grand Island, NY, USA). All data were normalized to *actinb1* expression and fold change was calculated using the  $2^{-\Delta\Delta Ct}$ .

### OT measurement

Wild-type and transgenic fish at 12 months of age were killed in 0.04% Tricaine (Sigma-Aldrich, St Louis, MO, USA). Brains were dissected, imaged and the OT from the midline to the left and right edges was measured and analyzed using Nikon NIS Elements. Data were analyzed using Microsoft Excel software and expressed as mean ± s.d. Significance was calculated by performing two-tailed Student's *t*-test and probability was set at *P* < 0.05.

### CONFLICT OF INTEREST

The authors declare no conflict of interest.

### ACKNOWLEDGEMENTS

We thank the late Dr Chi-Bien Chen for providing the Tol2 kit, Dr Patrick S Page-McCaw for critical comments and Ryan Gebert for excellent fish care. This research was supported by The Hartwell Foundation, St Jude Children's Research Hospital (SJCRH) and ALSAC. The SJCRH Cell & Tissue Imaging Center is supported by National Institutes of Health Grant NCI P30 CA021765-34.

### REFERENCES

- Ingham PW, Placzek M. Orchestrating ontogenesis: variations on a theme by sonic hedgehog. *Nat Rev Genet* 2006; **7**: 841–850.
- Ruiz i Altaba A, Palma V, Dahmane N. Hedgehog-Gli signalling and the growth of the brain. *Nat Rev Neurosci* 2002; **3**: 24–33.
- Schuller U, Heine VM, Mao J, Kho AT, Dillon AK, Han YG *et al*. Acquisition of granule neuron precursor identity is a critical determinant of progenitor cell competence to form Shh-induced medulloblastoma. *Cancer Cell* 2008; **14**: 123–134.
- Takezaki T, Hide T, Takanaga H, Nakamura H, Kuratsu J, Kondo T. Essential role of the Hedgehog signaling pathway in human glioma-initiating cells. *Cancer Sci* 2011; **102**: 1306–1312.
- Clement V, Sanchez P, de Tribolet N, Radovanovic I, Ruiz i Altaba A. HEDGEHOG-GLI1 signaling regulates human glioma growth, cancer stem cell self-renewal, and tumorigenicity. *Curr Biol* 2007; **17**: 165–172.
- Bar EE, Chaudhry A, Lin A, Fan X, Schreck K, Matsui W *et al*. Cyclopamine-mediated hedgehog pathway inhibition depletes stem-like cancer cells in glioblastoma. *Stem Cells* 2007; **25**: 2524–2533.
- Rush SZ, Abel TW, Valadez JG, Pearson M, Cooper MK. Activation of the Hedgehog pathway in pilocytic astrocytomas. *Neuro Oncol* 2010; **12**: 790–798.
- Ju B, Spitsbergen J, Eden CJ, Taylor MR, Chen W. Co-activation of hedgehog and AKT pathways promote tumorigenesis in zebrafish. *Mol Cancer* 2009; **8**: 40.
- Chua KL, Lim TM. Type I and type II cytokeratin cDNAs from the zebrafish (*Danio rerio*) and expression patterns during early development. *Differentiation* 2000; **66**: 31–41.

- Vihtelic TS, Fadool JM, Gao J, Thornton KA, Hyde DR, Wistow G. Expressed sequence tag analysis of zebrafish eye tissues for NEIBank. *Mol Vis* 2005; **11**: 1083–1100.
- Pierfelice TJ, Schreck KC, Eberhart CG, Gaiano N. Notch, neural stem cells, and brain tumors. *Cold Spring Harb Symp Quant Biol* 2008; **73**: 367–375.
- Chen W, Casey Corliss D. Three modules of zebrafish *Mind bomb* work cooperatively to promote Delta ubiquitination and endocytosis. *Dev Biol* 2004; **267**: 361–373.
- Lam CS, Marz M, Strahle U. *gfap* and *nestin* reporter lines reveal characteristics of neural progenitors in the adult zebrafish brain. *Dev Dyn* 2009; **238**: 475–486.
- Pisharath H, Rhee JM, Swanson MA, Leach SD, Parsons MJ. Targeted ablation of beta cells in the embryonic zebrafish pancreas using *E. coli* nitroreductase. *Mech Dev* 2007; **124**: 218–229.
- Lee J, Willer JR, Willer GB, Smith K, Gregg RG, Gross JM. Zebrafish blowout provides genetic evidence for Patched1-mediated negative regulation of Hedgehog signaling within the proximal optic vesicle of the vertebrate eye. *Dev Biol* 2008; **319**: 10–22.
- Bibliowicz J, Gross JM. Expanded progenitor populations, vitreo-retinal abnormalities, and Muller glial reactivity in the zebrafish *leprechaun/patched2* retina. *BMC Dev Biol* 2009; **9**: 52.
- Fulton AB, Craft JL, Howard RO, Albert DM. Human retinal dysplasia. *Am J Ophthalmol* 1978; **85**: 690–698.
- Lee KC, Goh WL, Xu M, Kua N, Lunny D, Wong JS *et al*. Detection of the p53 response in zebrafish embryos using new monoclonal antibodies. *Oncogene* 2008; **27**: 629–640.
- Dakubo GD, Wang YP, Mazerolle C, Campsall K, McMahon AP, Wallace VA. Retinal ganglion cell-derived sonic hedgehog signaling is required for optic disc and stalk neuroepithelial cell development. *Development* 2003; **130**: 2967–2980.
- Schmitz M, Temme A, Senner V, Ebner R, Schwind S, Stevanovic S *et al*. Identification of SOX2 as a novel glioma-associated antigen and potential target for T cell-based immunotherapy. *Br J Cancer* 2007; **96**: 1293–1301.
- Pasca di Magliano M, Hebrok M. Hedgehog signalling in cancer formation and maintenance. *Nat Rev Cancer* 2003; **3**: 903–911.
- Dahmane N, Sanchez P, Gitton Y, Palma V, Sun T, Beyna M *et al*. The Sonic Hedgehog-Gli pathway regulates dorsal brain growth and tumorigenesis. *Development* 2001; **128**: 5201–5212.
- Feijoo CG, Onate MG, Milla LA, Palma VA. Sonic hedgehog (Shh)-Gli signaling controls neural progenitor cell division in the developing tectum in zebrafish. *Eur J Neurosci* 2011; **33**: 589–598.
- Cancer Genome Atlas Research Network. Comprehensive genomic characterization defines human glioblastoma genes and core pathways. *Nature* 2008; **455**: 1061–1068.
- Abe Y, Oda-Sato E, Tobiume K, Kawauchi K, Taya Y, Okamoto K *et al*. Hedgehog signaling overrides p53-mediated tumor suppression by activating Mdm2. *Proc Natl Acad Sci USA* 2008; **105**: 4838–4843.
- Stecca B, Ruiz i Altaba A. A GLI1-p53 inhibitory loop controls neural stem cell and tumour cell numbers. *EMBO J* 2009; **28**: 663–676.
- Rebetz J, Tian D, Persson A, Widegren B, Salford LG, Englund E *et al*. Glial progenitor-like phenotype in low-grade glioma and enhanced CD133-expression and neuronal lineage differentiation potential in high-grade glioma. *PLoS ONE* 2008; **3**: e1936.
- Ben-Porath I, Thomson MW, Carey VJ, Ge R, Bell GW, Regev A *et al*. An embryonic stem cell-like gene expression signature in poorly differentiated aggressive human tumors. *Nat Genet* 2008; **40**: 499–507.
- Black GC, Mazerolle CJ, Wang Y, Campsall KD, Petrin D, Leonard BC *et al*. Abnormalities of the vitreoretinal interface caused by dysregulated Hedgehog signaling during retinal development. *Hum Mol Genet* 2003; **12**: 3269–3276.
- Moshiri A, Reh TA. Persistent progenitors at the retinal margin of *ptc+/-* mice. *J Neurosci* 2004; **24**: 229–237.
- Ragge NK, Salt A, Collin JR, Michalski A, Farndon PA. Gorlin syndrome: the PTCH gene links ocular developmental defects and tumour formation. *Br J Ophthalmol* 2005; **89**: 988–991.
- Roy S, Ingham PW. Hedgehogs tryst with the cell cycle. *J Cell Sci* 2002; **115**: 4393–4397.
- Wallace VA. Proliferative and cell fate effects of Hedgehog signaling in the vertebrate retina. *Brain Res* 2008; **1192**: 61–75.
- Sakagami K, Gan L, Yang XJ. Distinct effects of Hedgehog signaling on neuronal fate specification and cell cycle progression in the embryonic mouse retina. *J Neurosci* 2009; **29**: 6932–6944.
- Locker M, Agathocleous M, Amato MA, Parain K, Harris WA, Perron M. Hedgehog signaling and the retina: insights into the mechanisms controlling the proliferative properties of neural precursors. *Genes Dev* 2006; **20**: 3036–3048.
- Prykhodzhiy SV. In the absence of Sonic hedgehog, p53 induces apoptosis and inhibits retinal cell proliferation, cell-cycle exit and differentiation in zebrafish. *PLoS ONE* 2010; **5**: e13549.

- 37 Monje M, Mitra SS, Freret ME, Raveh TB, Kim J, Masek M et al. Hedgehog-responsive candidate cell of origin for diffuse intrinsic pontine glioma. *Proc Natl Acad Sci USA* 2011; **108**: 4453–4458.
- 38 Gruber Filbin M, Dabral SK, Pazyra-Murphy MF, Ramkissoon S, Kung AL, Pak E et al. Coordinate activation of Shh and PI3K signaling in PTEN-deficient glioblastoma: new therapeutic opportunities. *Nature Med* 2013; **19**: 1518–1523.
- 39 Gilley J, Fried M. One INK4 gene and no ARF at the Fugu equivalent of the human INK4A/ARF/INK4B tumour suppressor locus. *Oncogene* 2001; **20**: 7447–7452.
- 40 Grandel H, Kaslin J, Ganz J, Wenzel I, Brand M. Neural stem cells and neurogenesis in the adult zebrafish brain: origin, proliferation dynamics, migration and cell fate. *Dev Biol* 2006; **295**: 263–277.
- 41 Lillo C, Velasco A, Jimeno D, Cid E, Lara JM, Aijon J. The glial design of a teleost optic nerve head supporting continuous growth. *J Histochem Cytochem* 2002; **50**: 1289–1302.
- 42 Ruiz i Altaba A, Sanchez P, Dahmane N. Gli and hedgehog in cancer: tumours, embryos and stem cells. *Nat Rev Cancer* 2002; **2**: 361–372.
- 43 Listernick R, Ferner RE, Liu GT, Gutmann DH. Optic pathway gliomas in neurofibromatosis-1: controversies and recommendations. *Ann Neurol* 2007; **61**: 189–198.
- 44 Singhal S, Birch JM, Kerr B, Lashford L, Evans DG. Neurofibromatosis type 1 and sporadic optic gliomas. *Arch Dis Child* 2002; **87**: 65–70.
- 45 Dakubo GD, Beug ST, Mazerolle CJ, Thurig S, Wang Y, Wallace VA. Control of glial precursor cell development in the mouse optic nerve by sonic hedgehog from retinal ganglion cells. *Brain Res* 2008; **1228**: 27–42.
- 46 White RM, Cech J, Ratanasirinawoot S, Lin CY, Rahl PB, Burke CJ et al. DHODH modulates transcriptional elongation in the neural crest and melanoma. *Nature* 2011; **471**: 518–522.
- 47 Ridges S, Heaton WL, Joshi D, Choi H, Eiring A, Batchelor L et al. Zebrafish screen identifies novel compound with selective toxicity against leukemia. *Blood* 2012; **119**: 5621–5631.
- 48 Kwan KM, Fujimoto E, Grabher C, Mangum BD, Hardy ME, Campbell DS et al. The Tol2kit: a multisite gateway-based construction kit for Tol2 transposon transgenesis constructs. *Dev Dyn* 2007; **236**: 3088–3099.



*Oncogenesis* is an open-access journal published by Nature Publishing Group. This work is licensed under a Creative Commons Attribution-NonCommercial-ShareAlike 3.0 Unported License. The images or other third party material in this article are included in the article's Creative Commons license, unless indicated otherwise in the credit line; if the material is not included under the Creative Commons license, users will need to obtain permission from the license holder to reproduce the material. To view a copy of this license, visit <http://creativecommons.org/licenses/by-nc-sa/3.0/>

Supplementary Information accompanies this paper on the *Oncogenesis* website (<http://www.nature.com/oncsis>).